

PAPER • OPEN ACCESS

## Dependence of $V_2O_5$ Nanorods Properties on Substrate Type Prepared by Simple Hydrothermal Method

To cite this article: N.M. Abd-Alghafour *et al* 2020 *J. Phys.: Conf. Ser.* **1535** 012046

View the [article online](#) for updates and enhancements.



**IOP | ebooks™**

Bringing together innovative digital publishing with leading authors from the global scientific community.

Start exploring the collection—download the first chapter of every title for free.

# Dependence of V<sub>2</sub>O<sub>5</sub> Nanorods Properties on Substrate Type Prepared by Simple Hydrothermal Method

N.M. Abd-Alghafour<sup>1,2\*</sup>, Ghassan Adnan Naeem<sup>3</sup>, Sabah M. Mohammad<sup>4</sup>

<sup>1</sup>Iraqi Ministry of Education, Al-Anbar, Iraq

<sup>2</sup>University Of Anbar, College of Applied Sciences, Al-Anbar, Iraq

<sup>3</sup>Biophysics Department, College of Applied Science, University of Anbar

<sup>4</sup>Institute of Nano Optoelectronics Research and Technology (INOR), Universiti Sains Malaysia, 11800 USM, Penang, Malaysia

\*na2013bil@gmail.com

**Abstract.** V<sub>2</sub>O<sub>5</sub> (Vanadium pentoxide) nanorods were prepared onto various substrates by using simple hydrothermal method. The structural characteristics of the V<sub>2</sub>O<sub>5</sub> nanorods (NRs) have been examined via using XRD diffraction analysis. The effects of the various substrates on the morphological characteristics of V<sub>2</sub>O<sub>5</sub> NRs were investigated by using field emission scanning electron microscopy (FESEM) technique. The XRD results show that the preferred orientation along (001) plane. Raman spectra indicate that glass substrate has optimum results due to the size and number of the nanorods with lower defects. It can be found from the absorbance of the glass substrate increases compared with the other substrates.

## 1. Introduction

V<sub>2</sub>O<sub>5</sub> material has expanded interest because of their exceptional performance in optoelectronic, microelectronic and sensing applications [1]. The preparation of V<sub>2</sub>O<sub>5</sub> thin film by hydrothermal method has become an effective field because of its applications as sensors and catalyst devices. V<sub>2</sub>O<sub>5</sub> has direct bandgap of 2.3 eV which is use for photo-detection applications [2]. In the recent times, V<sub>2</sub>O<sub>5</sub> nanostructures such as nanowires [3], nanobelts [4], nanocolumnar [5], nanoporous [6], and nanorods [7] have gained an extensive attention due to interest properties such as Multivalancy, good chemical, thermal stability, and wide bandgap [8, 9]. Therefore, V<sub>2</sub>O<sub>5</sub> nanostructures (1D) are more suitable for applications of devices than other forms. Among these forms, V<sub>2</sub>O<sub>5</sub> NRs can be introduced into many applications in photo-detection devices and chemical sensing such as solar cells [10], infrared detectors [11], visible photodetector [12], gas sensor [13], and extended gate field effect transistor [14].

V<sub>2</sub>O<sub>5</sub> NRs can be prepared on various types of substrates by a several techniques such as atomic layer chemical vapor deposition (ALCVD) [15], thermal oxidation method [16], heating process [17], microwave-assisted hydrothermal [18], electron beam irradiation [19], sol electrophoretic deposition [20], spray pyrolysis technique [21], and simple hydrothermal method [22]. However, these processes obtained oxygen vacancies which influence on the vanadium oxidation and consequent surface reactivity considerably. Therefore, hydrothermal method has been chosen for the growth of V<sub>2</sub>O<sub>5</sub> NRs due to



numerous benefits such as low cost, effectively large area depositions, relatively simple and can be controlled the deposition parameters which lead to controlling their morphology [23]. In this work, we have studied the influence of the substrate type on the  $V_2O_5$  NRs properties by using hydrothermal method.  $V_2O_5$  NRs were successfully prepared on various substrates and have been investigated of the properties. XRD diffraction analysis, field emission scanning electron microscopy (FESEM), and Raman spectroscopy system were utilized to investigation the structural characteristics. The optical characteristics were investigated by using ultraviolet-visible technique.

## 2. Experimental

$V_2O_5$  NRs were deposited by using simple hydrothermal technique onto Si(100), glass, and ITO substrates. The silicon substrates were cleaned via using the American Radio Corporation cleaning method [24]. The glass microscope slides were divided into (2.5 cm × 2.5 cm) small square shapes before cleaning. These were cleaned by using beaker containing acetone solution. The beaker was ultrasonically cleaned for 15 mins. Then, the substrates were submerged in the beaker containing ethanol solution and ultrasonically cleaned for another 15 mins. Finally, the slides of glass were washed in the deionized water and dried with the nitrogen gas. In a typical growth of  $V_2O_5$  NRs, an orange solution containing 0.585 g ammonium met-vanadate ( $NH_4VO_3$ ) and 1.1206 g oxalic acid ( $H_2C_2O_4$ ) dissolved in distilled water of 50 ml instantly. The result mixture was stirred for 15 min under room temperature. After that 10 drop of the HCl was added. The prepared precursor was transferred into a glass bottle with the substrates and was kept at 95 °C for 3.5 h. At room temperature, all the substrates were rinsed with distilled water and dried in ambient air. The samples were annealed for 1 hour at 300 °C then 2 hour at 500 °C to generate a  $V_2O_5$  NRs.

## 3. Results and discussion

### 3.1 Structural properties

XRD result peaks of  $V_2O_5$  NRs deposited onto various substrates using simple hydrothermal technique are revealed in Figure 1. These peaks observed at  $2\theta = 20.23^\circ, 26.29^\circ, 27.78^\circ, 29.28^\circ, 30.77^\circ, 32.88^\circ, 41.18^\circ,$  and  $50.62^\circ$  are matched to the (001), (110), (101), (011), (301), (002), and (020) orientation planes. These XRD peaks confirm the composition of the orthorhombic structure according to the standard card JCPDS No.00-041-1426 [25]. XRD sharp peak is along (001) plane for glass and Si substrates because of low surface energy. The low peak is along (001) of the ITO substrate due to defects in the crystalline structure [26].  $V_2O_5$  NRs prepared on the glass substrate has higher intensity as compared with other substrates, which means that the enhancement the crystallinity and larger grain size [33].

This crystallinity can be attributed to the surface diffusion and activation of certain surface reactions. The size of crystallite was calculated along the corresponding XRD peak (001) using the relation as follow [27]:

$$D = \frac{k\lambda}{\beta \cos \theta} \quad (1)$$

In this relation D is the crystallite size,  $\lambda$  is the wavelength of the XRD radiation,  $\beta$  is the full width and half maximum (FWHM),  $\theta$  is angle in radians. The results indicate that the glass substrate has good value of crystallite size as compared to other substrates. The results shown that the enhancement the crystallinity and increasing of XRD diffraction peak of  $V_2O_5$  NRs [5]. The lattice constant have been calculated along of (001) plane. It was indicated that the value of lattice constant at glass substrate is consistent with the according to the standard card JCPDS No.00-041-1426 [25]. The results can be attributed to prepared

$V_2O_5$  NRs onto glass substrate has a low structural defect and improved the crystallization along (001) plane. The positive value of the strain indicated that the strain was tensile in nature. The determined of crystallite size values of  $V_2O_5$  NRs and FWHM are shown in Table 1.

**Table 1.** Measured values of the XRD analysis of  $V_2O_5$  NRs grown on the glass different substrates.

Substrate type	(001) 2 $\theta$ (°)	Lattice Constants c (Å)	FWHM (01) (°)	$\epsilon_c$ %	D (nm)
Si	20.232	4.390	0.275	0.297	29.335
glass	20.259	4.383	0.167	0.16	48.309
ITO	20.176	4.351	1.422	0.571	5.680

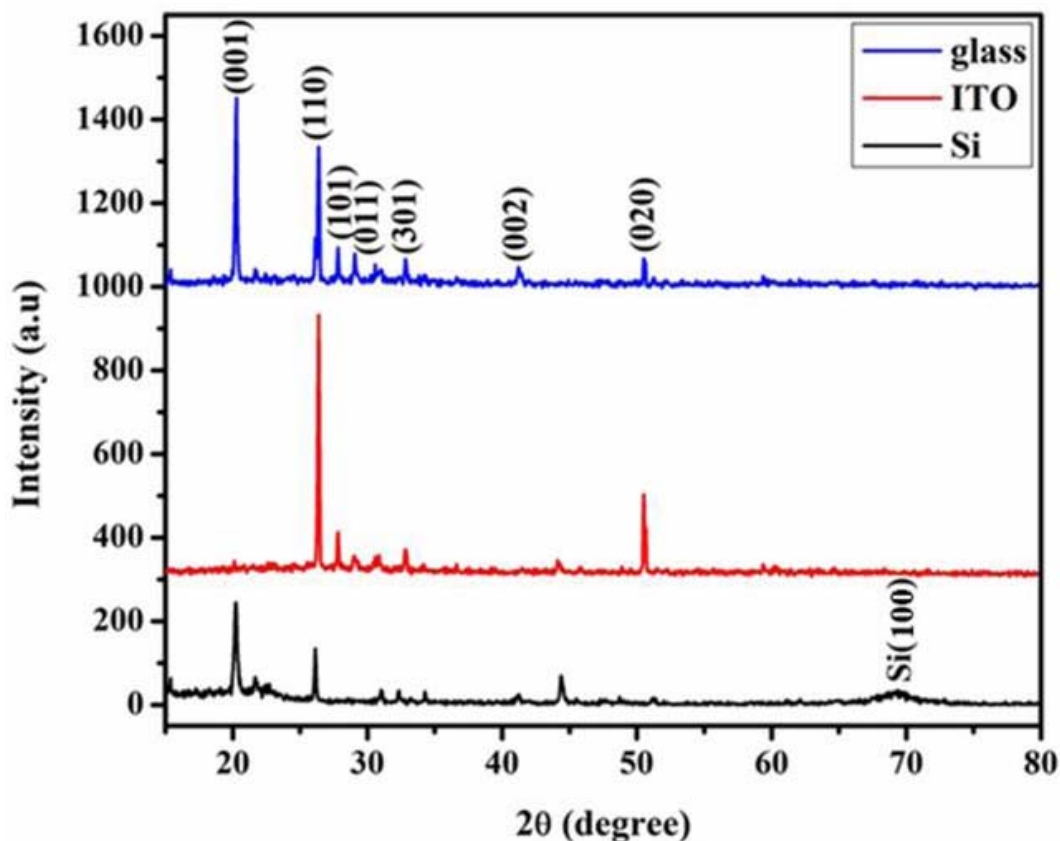


**Figure 1.** XRD patterns of  $V_2O_5$  NRs grown on the different substrates.

The Raman results of prepared  $V_2O_5$  NRs onto various substrates are shown in Figure 2. The result indicated that the Raman spectrum was symmetrical with Raman modes of  $V_2O_5$  structure [28]. The predominant peak at  $143\text{ cm}^{-1}$  wavenumber is associated to  $B_{3g}$  mode of V-O-V chains, which existence indicates layer structure of  $V_2O_5$  material.  $V_2O_5$  NRs prepared onto glass substrate have a (001) preferred

orientation along the c-direction perpendicular to the plane. The Raman spectrum peak at  $993\text{ cm}^{-1}$  wavenumber was related to the  $A_g$  vibration mode of the terminal oxygen (V=O) stretching mode which shortest vanadium oxygen bond [29]. The peaks located at  $405\text{ cm}^{-1}$  and  $282\text{ cm}^{-1}$  wavenumber are related to the bending vibration of the V=O bonds. The peaks at  $480\text{ cm}^{-1}$  and  $302\text{ cm}^{-1}$  wavenumber are related to the bending vibrations of the V-O-V and  $V_3$ -O bonds [30]. The  $V_3$ -O stretching mode was observed at  $519\text{ cm}^{-1}$  which results from edge-shared oxygens in common to three-pyramids. The peak centred at  $694\text{ cm}^{-1}$  is associated to the  $V_2$ -O stretching mode which results from corner shared oxygens in common to two-pyramids [31]. However, the Raman spectra are in good agreement with the XRD results.

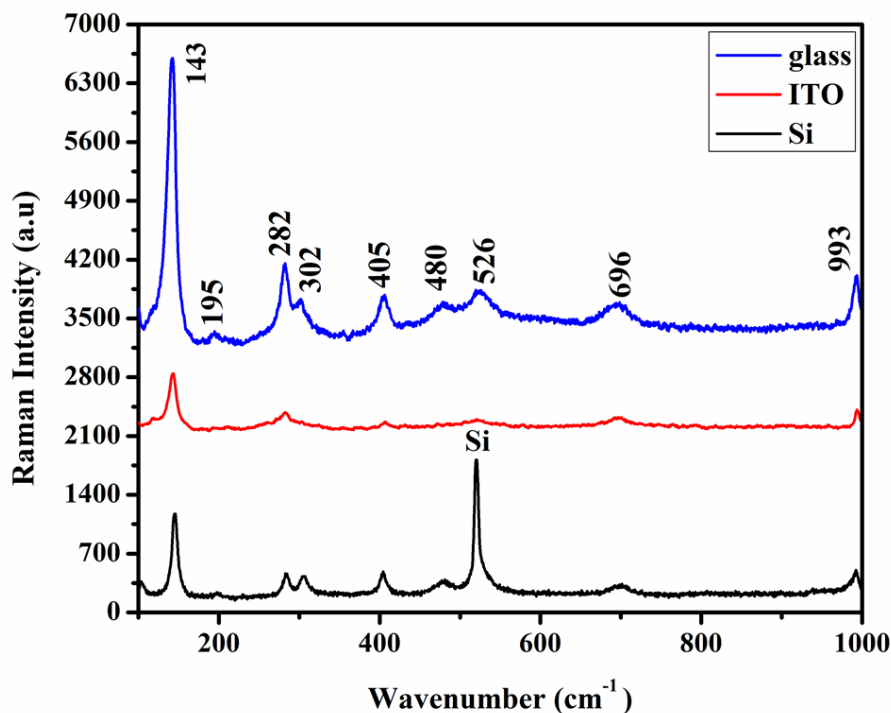


**Figure 2.** Raman spectra of  $V_2O_5$  NRs grown on the different substrates.

### 3.2. FESEM observation

Figure 3 shows the surface morphology of  $V_2O_5$  NRs prepared onto different substrates. The images indicate high size and density of nanorods and uniform growth which is vertically aligned on the substrates with an orthorhombic structure. The nanorods grown on the Si substrate are typically around 170 nm in length and 70-90 nm in diameter, as shown in Figure 3(a). At the ITO substrate, the diameter of the nanorods is obvious in the 100-120 nm diameter range. At glass substrate as revealed in Figure 3(c-d), the  $V_2O_5$  nanorods have the average lengths of 400-600 nm and diameters of 40-60 nm due to grow the nanorods from vapour of the material droplets passing near to the substrate during the evaporation process. The nucleation locations number increases when the substrates coverage is completed with high density nanorods. The nucleation sites functioned as a base for collecting small particles. As the grains agglomerate, the active nucleation sites of  $V_2O_5$  grains disorientate, resulting in  $V_2O_5$  NRs growth orientation [32].

### 3.3. Optical properties

Figure 4 displays the absorbance spectra of  $V_2O_5$  NRs prepared onto different substrates.  $V_2O_5$  NRs deposited on glass substrate indicated a higher absorbance value which showed the formation of  $V_2O_5$  NRs with enhanced crystalline nature. The results indicated that the exciton absorbance peak at 2.48 eV (498 nm) which displays a blue shift as compared with the bulk value of  $V_2O_5$  (2.3 eV). It can be attributed to the electrons transition from the O2p valence band to the V3d conduction band of vanadium atoms [33]. The transition band ( $O \rightarrow V^{n+}$ ) of the charges associated to the oxygen atoms around the vanadium ion. Hence, vanadium ion ( $V^{5+}$ ) in octahedral form absorbs at 450-600 nm wavelength. The results indicate a low absorbance peak at wavelength of 498 nm which is attributed to lower energy charge transfer to  $V^{5+}$  species in octahedral form. Moreover, the absorbance peak of  $V_2O_5$  NRs shows a blue shift at glass substrate which attributes the decrease of the bandgap of the samples.

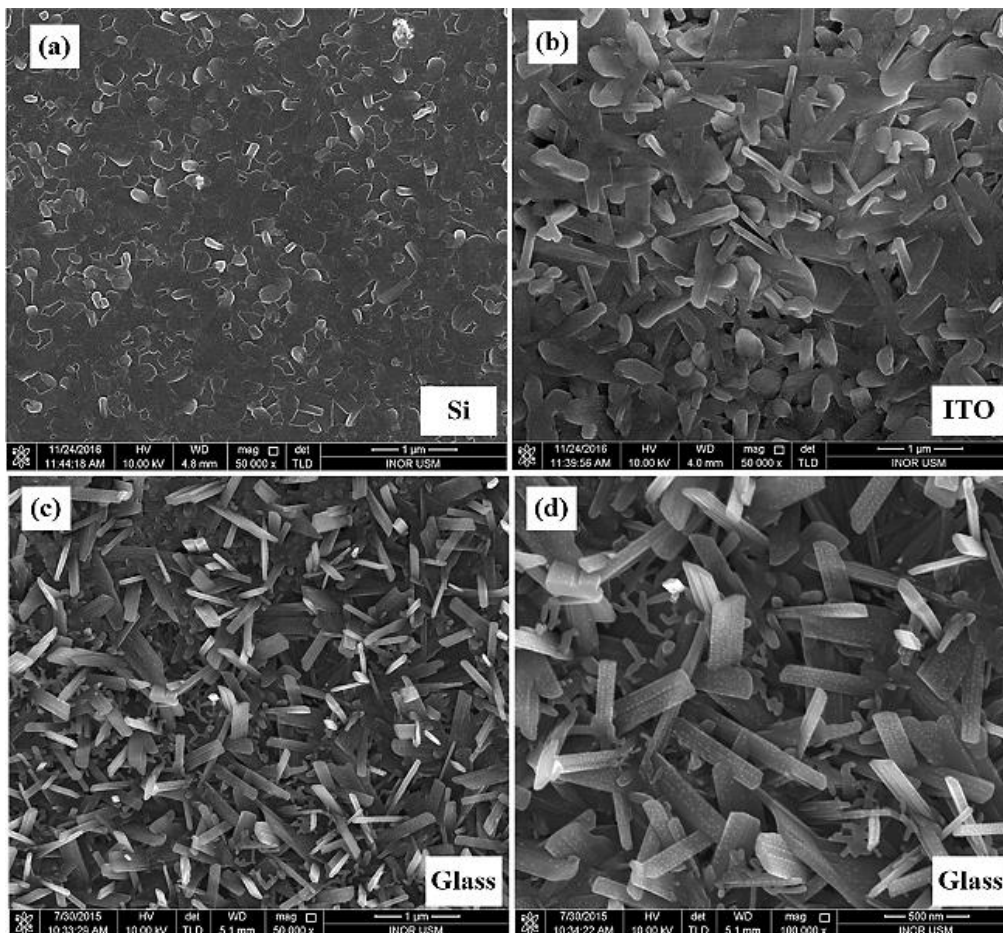


**Figure 3.** FESEM images of  $V_2O_5$  NRs grown on the different substrates.

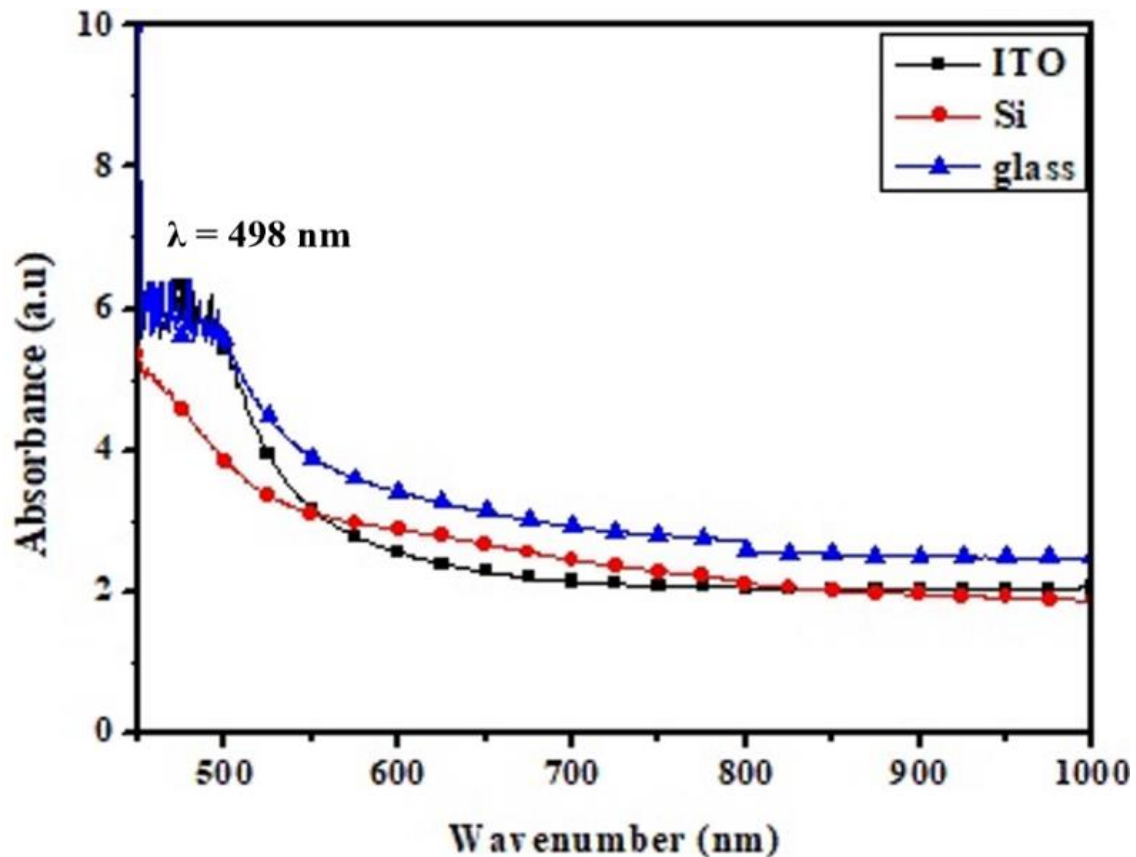


Figure 4. Optical absorbance spectra of  $V_2O_5$  grown on the different substrates.

#### 4. Conclusion

$V_2O_5$  NRs high density was prepared on different substrates types by using simple hydrothermal method. The XRD results indicate enhancement the crystallinity and larger grain size under glass substrate. A Raman spectrum shows symmetric with the Raman modes of the  $V_2O_5$  structure. The FESEM images indicate high size and density of nanorods and uniform growth which is vertically aligned on the substrates with an orthorhombic structure. The absorbance peak of  $V_2O_5$  NRs shows a blue shift at glass substrate which attributes the decrease of the bandgap of the sample grown onto glass substrate.

#### Acknowledgments

This work has been partly supported by the Iraqi Ministry of Education, the Iraqi Ministry of Higher Education and Scientific Research, University of Anbar and Bridging grant-USM (304.CINOR.6316526).

#### References

- [1] Zhai T, Liu H, Li H, Fang X, Liao M, Li L, Zhou H, Koide Y, Bando Y and Golberg D 2010 *Adv. Mat.* **22** 2547-52
- [2] Kim B H, Kim A, Oh S Y, Bae S S, Yun Y J and Yu H Y 2008 *Appl. Phys. Lett.* **93** 233101-04
- [3] Chen R S, Wang W C, Chan C H, Hsu H P, Tien L C and Chen Y J 2013 *Nanoscale Res. Lett.* **8** 443-51

- [4] Sharma R K, Kumar P and Reddy G 2015 *J. Alloys Compd.* **638** 289-97
- [5] Raj D V, Ponpandian N, Mangalaraj D and Viswanathan C 2013 *Mat. Sci. Semicon. Proc.* **16** 256-62
- [6] Kong L and Taniguchi I 2016 *J. Power Sources* **312** 36-44
- [7] Hu Y, Li Z, Zhang Z, Meng D 2009 *Appl. Phys. Lett.* **94** 103107-10
- [8] Akl A A 2010 *J. Phys. Chem. Solids* **71** 223-229
- [9] Abyazisani M, Bagheri-Mohagheghi M M, Benam M R 2015 *Mat Sci Semicon Proc.* **31** 693-99.
- [10] Almora O, Gerling L G, Voz C, Alcubilla R, Puigdollers J, Garcia-Belmonte G 2017 *Sol. Energy Mat. Sol. C* **168** 221-26
- [11] Kumar P R, Karunakaran B, Mangalaraj D, Narayandass S K, Manoravi P, Joseph M, Gopal V, Madaria R and Singh J 2003 *Mater. Res. Bull.* **38** 1235-40
- [12] Pawar M S, Bankar P K, More M A and Late D J 2015 *RSC Adv.* **5** 88796-804
- [13] Modafferi V, Trocino S, Donato A, Panzera G and Neri G 2013 *Thin Solid Films* **548** 689-94
- [14] Guerra E M, Silva G R and Mulato M 2009 *Solid State Sci.* **11** 456-60
- [15] Groult H, Balnois E, Mantoux A, Le Van K, Lincot D 2006 *Appl. Surf. Sci.* **252** 5917-25
- [16] Wang Y, Li Z, Sheng X and Zhang Z 2007 *J. Chem. Phys.* **126** 164701-03
- [17] Yan W, Hu M, Wang D and Li C 2015 *Appl. Surf. Sci.* **346** 216-22
- [18] Pan J, Li M, Luo Y, Wu H, Zhong L, Wang Q and Li G 2016 *Mater. Res. Bull.* **74** 90-5
- [19] Kang M, Chu M, Kim S W and Ryu J W 2013 *Thin Solid Films* **547** 198-201
- [20] Takahashi K, Wang Y and Cao G 2005 *Appl. Phys. Lett.* **86** 053102-04
- [21] Mane A, Ganbavle V, Gaikwad M, Nikam S, Rajpure K and Moholkar A 2015 *J Anal Appl Pyrol.* **115** 57-65
- [22] Mu J, Wang J, Hao J, Cao P, Zhao S, Zeng W, Miao B and Xu S 2015 *Ceramics Int.* **41** 12626-32
- [23] Patil U, Kulkarni S, Deshmukh P, Salunkhe R and Lokhande C 2011 *J Alloy Compd.* **509** 6196-99
- [24] Al-Hardan N, Abdullah M and Aziz A A 2013 Performance of Cr-doped ZnO for acetone sensing *Appl. Surf. Sci.* **270** 480-485
- [25] Qin Y, Fan G, Liu K and Hu M 2014 *Sensor Actuat. B-Chem.* **190** 141-8
- [26] Thiagarajan S, Thaiyan M, Ganesan R 2015 *New J. Chem.* **39** 9471-9
- [27] Moholkar A, Pawar S, Rajpure K Y, Almari S N, Patil P and Bhosale C 2008 *Sol. Energ. Mat. Sol. C* **92** 1439-1444
- [28] Bouzidi A, Benramdane N, Bresson S, Mathieu C, Desfeux R and El Marssi M 2011 *Vib. Spectrosc.* **57** 182-6
- [29] Julien C, Haro-Poniatowski E, Camacho-Lopez M, Escobar-Alarcon L and Jimenez-Jarquín J 1999 *Mater. Sci. Eng. B* **65** 170-6
- [30] Lee S H, Cheong H M, Seong M J, Liu P, Tracy C E, Mascarenhas A, Pitts J R and Deb S K 2003 *Solid State Ion.* **165** 111-6
- [31] Chen W, Mai L, Peng J, Xu Q and Zhu Q *Solid State Chem.* **177** 377-9
- [32] Selman A M and Hassan Z 2015 *Sensor Actuat. A Phys.* **221** 15-21
- [33] Talledo A and Granqvist C G 1995 *J. Appl. Phys* **77** 4655-66